LBL--27267

DE89 014893

States of Oxygen Ordering in $YBa_2Cu_3O_z$

D. de Fontaine

Department of Materials Science and Mineral Engineering
University of California

and

Materials and Chemical Science Division
Lawrence Berkeley Laboratory
1 Cyclotron Road
Berkeley, California 94720

May 1989

STATES OF OXYGEN ORDERING IN $YBa_2Cu_3O_z$

D. de Fontaine

Department of Materials Science
and Mineral Engineering
University of California
Berkeley, CA 94720

INTRODUCTION

The compound $YBa_2Cu_3O_z$ (1-2-3) was the first one whose superconducting transition temperature exceeded the technologically important temperature of 77K[1]. Actually, the 1-2-3 compound at close to oxygen stoichiometry z=7 became superconducting at about T_c=90K, with T_c dropping by increments as z decreased from the value 7.

In this compound, the transition temperature is closely related to the oxygen content but is also thought to be influenced by the arrangement of occupied and vacant oxygen sites in the CuO_2 mirror plane of the structure, i.e. the plane located between Ba ions. In the 90K superconducting phase, occupied sites form O-Cu-O chains, and the resulting three-dimensional structure has orthorhombic symmetry. When available sites in the mirror plane are occupied statistically by O ions, the resulting structure has tetragonal symmetry and the material is non-superconducting. It thus appears that the tetragonal to orthorhombic transition in the 1-2-3 compound can be modeled by an order-disorder transition in the mirror plane. It is the object of this paper to review the properties of this transition and to derive appropriate phase diagrams pertaining to oxygen ordering in the plane. Much pertinent information concerning oxygen ordering in 1-2-3 is reviewed in a recent paper by Beyers and Shaw[2].

THE MODEL

It follows from the foregoing that attention must be focussed on the mirror plane, a schematic representation of which is shown in Fig. 1[3]. Open circles denote oxygen sites which may be vacant or occupied; black dots refer to Cu ion positions, assumed to be always occupied. The oxygen sites form two

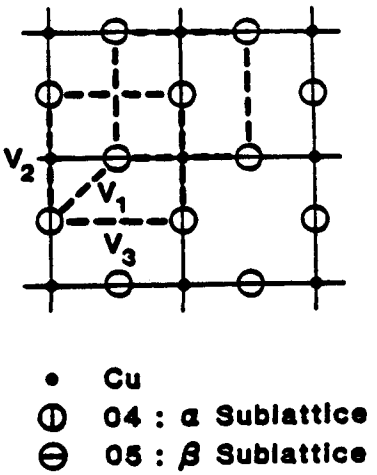

Fig. 1. Model for perovskite mirror plane with effective pair interactions V_n indicated.

interpenetrating square lattices and, if the Cu ions did not break the symmetry, the filled/empty oxygen network could be treated as a classical two-dimensional Ising model.

To simplify the thermodynamics, only three effective pair interactions (EPI) will be considered: V_1 which couples the two sublattices, V_2 which is a second neighbor interaction mediated by Cu, and V_3 which is the other next neighbor interaction. These three EPI's are expected to be the dominant ones.

EPI's are defined formally by

$$V_n = \frac{1}{4}(W_{OO}^{(n)} + W_{\square\square}^{(n)} - 2W_{O\square}^{(n)}) \qquad (n = 1,2,3)$$

where, for given pair spacing (n), $W_{IJ}^{(n)}$ represents the total energy of an otherwise disordered solution of O (oxygen) and $\square$ (vacancies) on the plane but containing the designated IJ pair at the specified sites. These energies can be calculated in principle by performing electronic band structure calculations. Such calculations have not yet been performed but plausibility arguments[4] indicate that V_1 must be positive, V_2 negative, of comparable magnitude, and V_3 negative but of lesser magnitude. From Eq. (1), it is seen that positive interactions favor unlike pairs, and negative interactions like pairs.

Several remarks concerning these EPI's are in order. Firstly, the V_n are *effective* interactions and must not be confused with *pair potentials*. Equation (1) clearly indicates that the EPI are calculated by taking differences of total energies. Actually, although pair potentials converge slowly with pair spacing, if at all, EPI's converge rapidly in metals[5], as if the long-range interactions canceled out by taking differences. Secondly, although the thermodynamic model proposed is a two-

dimensional one, the full three-dimensional character of the system is introduced in the V_n interactions. Finally, it is important to allow second neighbor asymmetry: $V_2 \neq V_3$. Other proposed models which assume $V_2=V_3$ are clearly deficient since they neglect the presence of Cu in the mirror plane, clearly a serious omission.

GROUND STATE ANALYSIS

Regardless of the values of the V_n's, it is instructive to perform a stability analysis of a completely disordered solid solution of oxygen and vacant sites. The second order term of a Landau expansion of the system's free energy in terms of amplitudes of oxygen "concentration waves" must have extrema at "special positions" in k-space which, in the present case, are points $\langle 0,0\rangle$, $\langle 1/2,0\rangle$ and $\langle 1/2,1/2\rangle$.[3] Which of these points present an actual minimum depends on the ratios $x=V_2/V_1$ and $y=V_3/V_1$. Results of the stability analysis are shown in Fig. 2: in each sector of the (x,y) plane is indicated which special point produces a free energy minimum. In particular, the $\langle 0,0\rangle$ special point indicates that an oxygen/vacancy wave of infinite wavelength modulates one of the sublattices and another, 180° out of phase with the first (because of $V_1>0$) modulates the other sublattice. In other words, one sublattice is filled by oxygen atoms and the other remains empty. The familiar chain structure of the orthorhombic phase results.

Actual ground states of order can also be investigated for all possible values of the ratios x, y. The results are indicated in Fig. 3[6]. For this range of EPI's, ordered structures are found only at stoichiometries $c_o=1/2$ or $1/4$ (or $3/4$), where c_o is the oxygen atom fraction in the mirror plane. In Fig. 3a ($c_o=1/2$), the familiar chain structure is depicted in the $\langle 0,0\rangle$ instability region. More complicated structures are found in other regions but for x,y ratios which are not relevant to the present system according to the qualitative discussion given above. At $c_o=1/4$, complete phase separation is predicted for (x,y) in the fourth quadrant (Fig. 3b), and two new cell doubling structures (p2mm) are found in the second and third quadrants. Actually, the structure with "b" O-Cu-O and ❑-Cu-❑ chain alternating along "a" has been observed experimentally in $YBa_2Cu_3O_z$ for $z\cong 6.5$[7-13], which corresponds to $c_o=1/4$ if it is assumed that all oxygen depletion occurs within the mirror plane. Clearly, if the EPI's are weakly dependent on concentration, the conditions for stability at low temperatures for both the single-chain structure, now called Ortho I, and the alternating chain structure, now called Ortho II, are $V_1>0$, $V_2<0$ and $0<V_3<\frac{1}{2}V_1$.

PHASE DIAGRAMS

The basic premise on which the present model rests is that the true three-dimensional order-disorder (oxygen-vacancy) phase transformations which occur in $a_2Cu_3O_z$ can be mapped onto a two-dimensional Ising model which is isotropic in the first-neighbor interactions and anisotropic in the second-neighbor interactions. The two-dimensional Ising model on a square lattice with first-neighbor interaction in zero field can be solved exactly but, when higher interactions are introduced, or when the applied field (magnetic, chemical potential difference) is non-zero, no closed form solution exists so that approximate methods must be used. Square lattice phase diagrams for first and second neighbor interactions have been

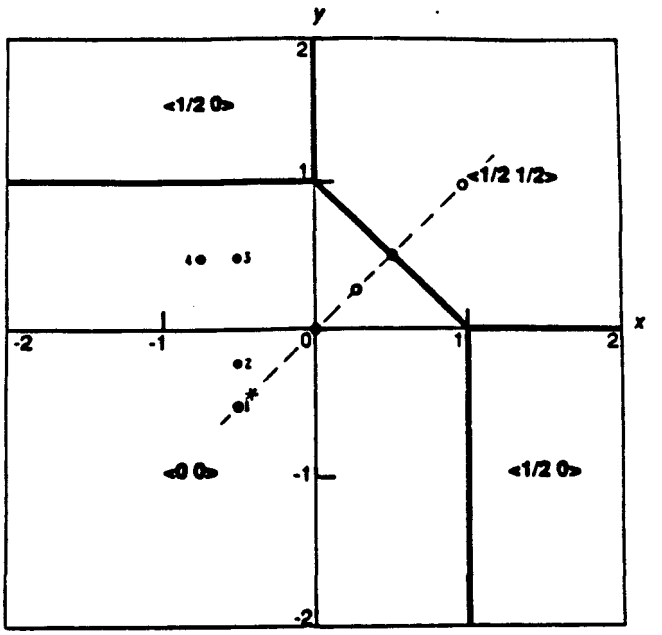

Fig. 2. Ordering instability map for $V_1>0$ (ordering first-neighbor interaction Coordinates are the ratios $x=V_2/V_1$, $y=V_3/V_1$. Open circles indicate parameter ratios for which phase diagrams were calculated previously by other methods. Closed circles (numbered) indicate parameters chosen for present calculations.

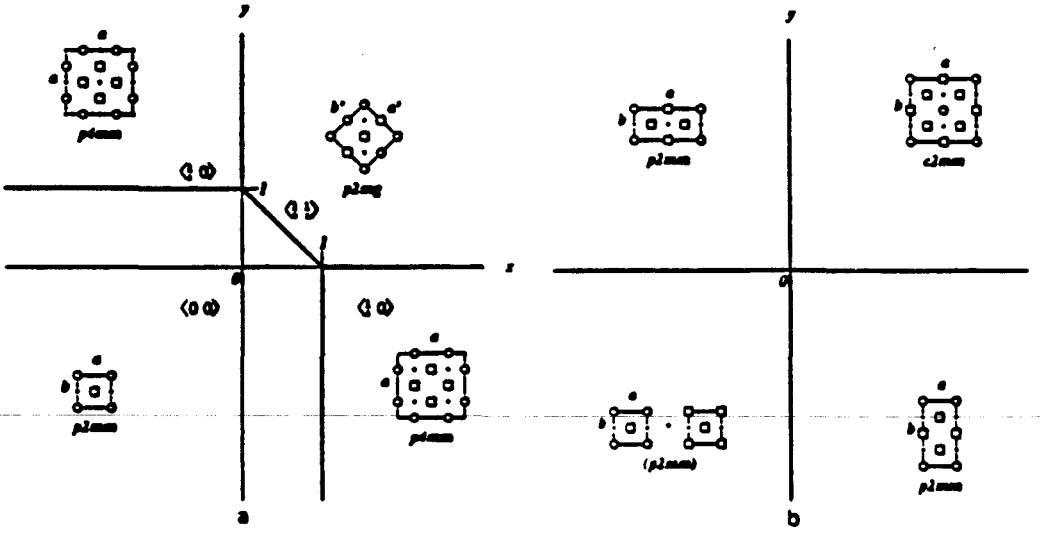

Fig. 3. Ground states as a function of $x=V_2/V_1$, $y=V_3/V_1$, at oxygen concentration: (a) 0.50 (b) 0.25.

calculated previously by renormalization group[14] and Monte Carlo[15] techniques. Recently[16,17], it was found that the suggested assymmetric model belonged to the same universality class as the Ashkin-Teller model[18] for which certain global phase diagrams have been derived[19]. This latter model considers a square lattice whose sites may be occupied by four types of objects in equal abundance with two distinct EPI's: one between like and one between unlike neighbors.

For the present calculations, the cluster variation method (CVM) of Kikuchi[20] was adopted. First, a test case was computed, that corresponding to $V_2=V_3=-\frac{1}{2}V_1$ ($V_1>0$) since previous phase diagram calculations were available[14,15] for these "symmetric" values of parameters. Results of the calculation have been reported earlier[21] and details of the CVM applied to this case were described elsewhere[22]. The representative point characterizing this phase diagram in parameter space is shown in Fig. 2 as "point #1" by a dot (our calculations) inside an open circle (previous calculations pertaining to symmetric cases).

The CVM phase diagram agreed closely with renormalization group[14] and Monte Carlo[15] results: a line of second order transitions separates the disordered (Tetragonal, planar point group 4mm) from the ordered (Ortho I, planar point group mm) phases and this line terminates at a tricritical point below which complete phase separation occurs. For the renormalization group and Monte Carlo calculations, the second-order transition line tends to be steeper just above the tricritical point and the top of the miscibility gap is also flatter than it is for the CVM calculations. The latter discrepancy is due to the fact that the CVM is, itself, a mean field theory, though a considerably improved one, and it tends to give classical exponents at transitions. It is known, however, that tricritical exponents are highly non-classical in two-dimensions.

CVM calculations performed for parameter ratios at point #2 on the stability map (Fig. 2), away from the diagonal x=y, produce a phase diagram which is very similar to that described above, and requires no further discussion. When V_3 is made to change from negative to small positive values, however, qualitative changes occur: a cell doubling phase, Ortho II, appears near stoichiometry $c_o=1/4$, as predicted by ground states analysis. Two phase diagrams have been computed with representative point #3 and #4 on the stability map.

The phase diagrams corresponding to point #4 is shown in Fig.4 [24]. In this figure, the phase boundary lines were terminated when the CVM free energy minimization failed to converge numerically. The most prominent feature of this diagram is the Ortho II phase region pertaining to a new, stable, equilibrium ordered phase, for which there is now ample experimental evidence.

Experimentally determined Tetra.↔ Ortho. I transition points have also been plotted on the phase diagram of Figs. 4 (closed circles). These points were constructed as follows: the data, obtained by a group from the Oak Ridge National Laboratory[25] give Tetra.↔ Ortho. I transition temperatures as a function of oxygen concentration at five different oxygen partial pressures. The data point for $p_{O_2}=0.2$

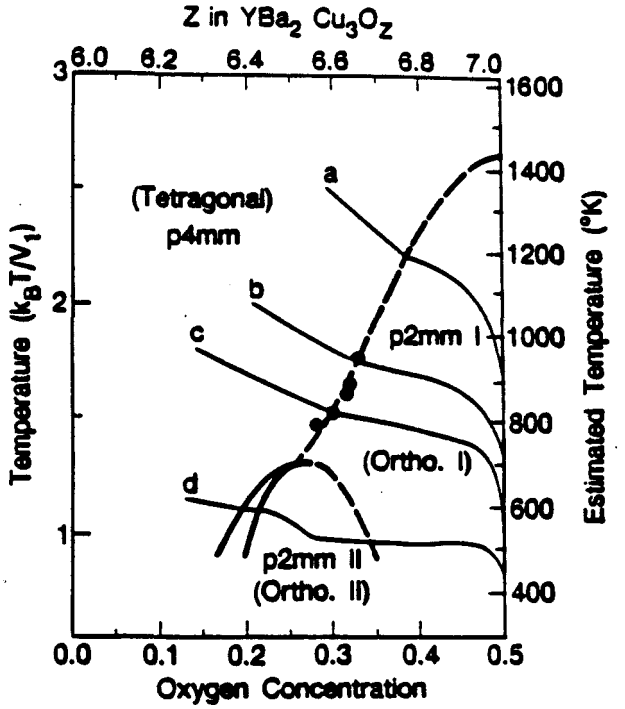

Fig. 4. Phase diagram calculated for x=–0.75, y=+0.50. Dashed lines are second order transitions, full lines are first order phase boundaries. Filled circles are order-disorder transition points determined experimentally (Ref. 25).

atm. was placed on the calculated order-disorder transition line, thereby fixing the temperature scale, i.e. fixing the value of the first EPI V_1. All other points at $5x10^{-3}$, 10^{-1}, $2x10^{-1}$ and 1 atm. then fell very nicely on the calculated curve. By this method, an estimated temperature scale could be constructed (right hand scale). An oxygen content scale, measured by the oxygen stoichiometry index z, is also shown at the top portion of Fig. 4. Oxygen partial pressure curves are also shown in Fig. 4; these were calculated by making use of two points from the Oak Ridge data, as explained elsewhere[24].

Very recently, Kikuchi and Choi[26] have extended to low temperatures our previous phase diagram calculation[27] for the case $V_2 = -0.5V_1$, $V_3 = +0.5V_1$ (point #3 in Fig. 2), thereby showing that our conjectured low temperature phase boundaries were incorrect. The Kikuchi-Choi (KC) phase diagram is reproduced in Fig. 5 (redrawn with our earlier temperature scales[27]) with four of the Oak Ridge data points shown. The superconductivity transition temperature as a function of oxygen content is also indicated (lower dashed curve). As in the earlier calculation[27], the line of second order Tetragonal (T) to Orthorhombic (OI) transition terminates in a bicritical point below which the Ortho. II (OII) phase is stable. The OI↔ OII transition is found to be second-order down to absolute zero of temperature while the T ↔ OII transition is first order. The upper dashed line is

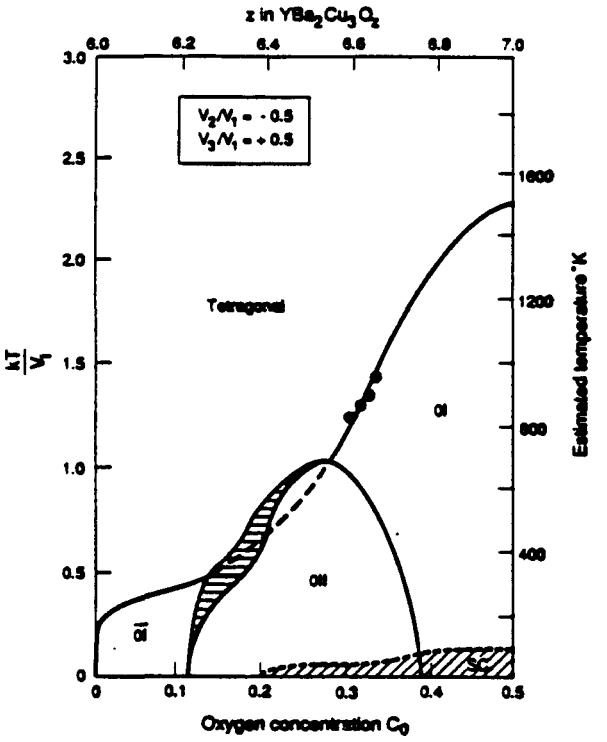

Fig. 5. CVM phase diagram according to Kikuchi and Choi (Ref. 26) calculated for x = –0.50, y = +0.50. Filled circles are order-disorder transition points determined experimentally (Ref. 25)

the metastable extension, though the OII phase region, of the T ↔ OI line of second order transitions. This line emerges from the OII region at a critical end point to produce an "anti-Ortho. I" ($\overline{OI}$) phase region at low temperatures and oxygen concentrations. The narrow two-phase region to the left of OII (horizontal shading) appears to terminate at a tricritical point at low temperature.

The OI phase has the well-known "chain" structure (lower left sector of Fig. 3a) with occasional missing oxygen rows. The $\overline{OI}$ phase is, in a sense, the converse: now the concentration of missing rows is much greater that that of filled rows. Between OI and $\overline{OI}$, OII is characterized by double-cell long range order (LRO) (upper left panel of Fig. 3b: every other chain missing). Phase $\overline{OI}$ differs from the Tetragonal (T) in that the former has parallel chain LRO on one sublattice only, T has fluctuating short chains on both oxygen sublattices, therefore along two orthogonal directions; T has tetragonal, $\overline{OI}$ has orthorhombic symmetry. At low enough temperature, an infinitesimal amount of oxygen will form long chains on a single sublattice, thereby breaking the tetragonal symmetry. Recent transfer matrix calculations[16] on the very same system indicate that the T ↔ OII transition is a second-order one with critical exponents depending on concentration, as in the

Ashkin-Teller model. The other transitions are confirmed to be Ising-like and second-order.

The 60K superconductivity transition temperature plateau shown in Fig. 5 fits fairly well inside the OII phase boundaries at around 400K, where the oxygen configurations must be "frozen in". This suggests that OII is indeed the observed 60K superconductor.

ONE-DIMENSIONAL STATES OF ORDER

Monte Carlo simulations were also performed[28,29] with the same EPI ratios, i.e. those corresponding to point #3 on the parameter map of Fig. 2. At high temperatures, agreement with previous CVM calculations[12] was quite satisfactory. At low temperature simulations, around $\tau \equiv k_B T/V_1 = 0.2$ ($k_B T$ has its usual "Boltzmann constant, absolute temperature" meaning), spurious specific heat maxima occurred in and around the OII phase field. Examination of computer printouts revealed that these specific heat anomalies corresponded to states of somewhat irregularly spaced parallel O-Cu-O chains.

A typical partially ordered structure is shown in Fig. 6a where black dots denote Cu atoms, shaded circles are oxygen atoms and open circles are vacant sites. This structure was obtained by performing a Monte Carlo simulation on a 64 x 64 square network of oxygen sites at fixed chemical potential field (normalized by V_1) of $\mu = -4.7$. Oxygen coverage in the plane is $c_o = 0.2265$ or stoichiometry index z = 6.453. The system was "quenched" from a high temperature of $\tau = 5.0$ and the iteration was pursued to 1200 Monte Carlo steps per site. O-Cu-O chains are seen to be fully formed and are stacked in such a way as to form regions of Ortho. II separated by slabs of "Ortho. III" (full-empty-empty-full cell tripling structure). The corresponding intensity pattern, i.e. the amplitude-squared of the Fourier transform, or oxygen structure factor of Fig. 6a, is shown in Fig. 6b. Diffraction maxima are located at <00>, <20> and <11> which are the "Bragg peaks" in planar reciprocal space notation, and at <10> which are the Ortho. I "reflections". The $\langle\frac{1}{2}0\rangle$ reflections are split into satellite peaks at $\langle\frac{1}{2}\pm q,0\rangle$, with q not necessarily a simple fraction. At an earlier stage of the simulation (500 Monte Carlo steps/site), the chains were often faulted and both α and β oxygen sublattice occupancy domains were observed (see Fig. 7). Chain formation dynamics is discussed in more detail by Burmester and Wille.[29]

Another mode of "sample preparation" also was used in the simulations: first Ortho. I was produced at $\mu = -2.0$, then oxygen was extracted by imposing a chemical potential field of $\mu = -3.2$., this procedure being equivalent to reducing the partial pressure of Oxygen. After 8000 Monte Carlo steps/site, a structure consisting of mixed Ortho. II and Ortho. I slabs was obtained as seen in Fig. 8. The average planar oxygen concentration was $c_o = 0.297$, corresponding to stoichiometry z = 6.594. Once again the chains were fully formed but the OI and OII mixing was rather irregular, giving rise to a diffraction pattern consisting of a diffuse streak centered on $\langle\frac{1}{2}0\rangle$ along the a direction. It is easy to rationalize how

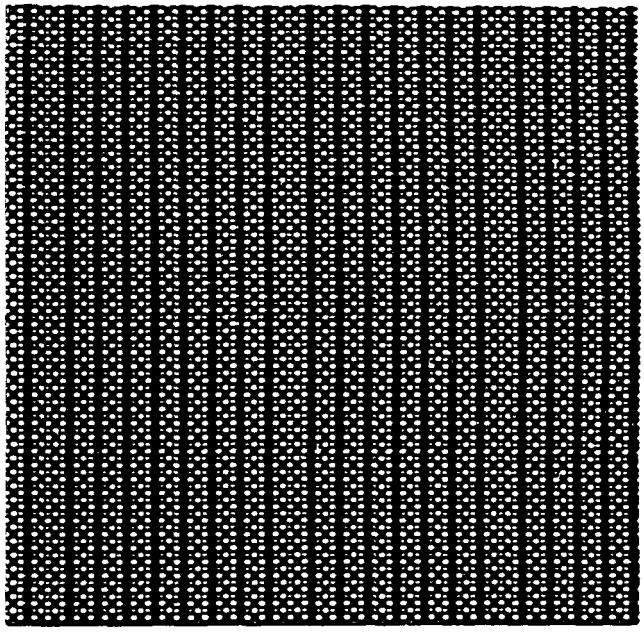

Fig. 6a. Chain configuration for Monte Carlo system quenched from $\tau = 0.2$ at constant $\mu = -4.7$, after 1200 Monte Carlo steps/site. Closed circles denote oxygen ions, open circles are vacant sites, and small dots (perhaps not readily visible) indicate Cu ions. Concentration is $c_O = 0.2265$ or oxygen stoichiometry index $z = 6.453$. Structure is one of mixed OII and $\overline{\text{OI}}$ domains.

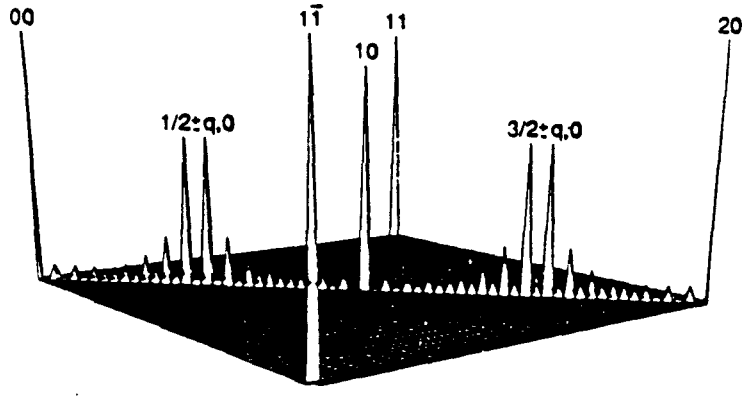

Fig. 6b. Fourier transform (amplitude squared) of configuration of Fig. 6a showing characteristic split (1/2, 0) peaks and (1,0) streaks of intensity.

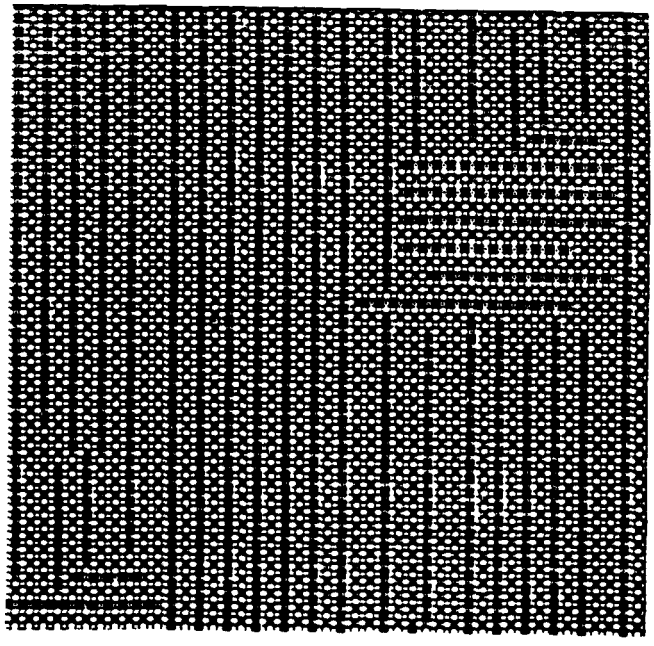

Fig. 7. Chain configuration for Monte Carlo system of Fig. 6a but at an early stage of iteration (500 Monte Carlo steps/site).

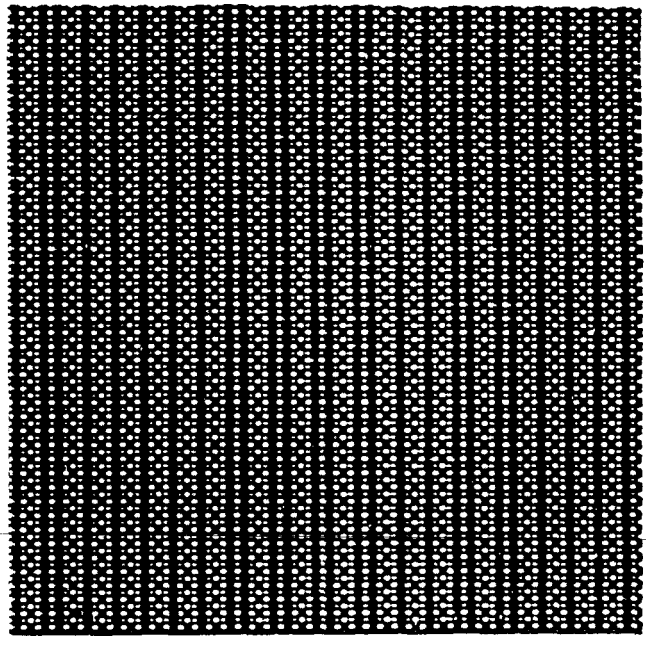

Fig. 8. Chain configuration for a Monte Carlo system initially in Ortho. I state, equilibrated at $\mu = -3.2$. Configuration is $c_o = 0.297$ or $z = 6.594$. Structure is one of mixed OI and OII domains.

such a structure could come about. Because of periodic boundary conditions, complete O-Cu-O chains are infinite and thus very robust. Eventually a chain is broken by action of the chemical potential field and it subsequently dissolves, thereby creating a slab of Ortho. II. The process is then repeated but in such a way that, at least for $c_0 > 0.25$, no two empty chains form adjacent to one another. The reason for that is as follows: fully formed chains on a single sublattice interact only through the effective V_3 interaction which is repulsive ($V_3 > 0$), thus favoring unlike nearest neighbor parallel chains. Hence a mixed state of OI and OII domains results. For $c_0 < 0.25$ ($z < 6.5$), the situation is slightly different: the mixing is between OII and $\overline{\text{OI}}$ domains.

This quasi one-dimensional admixture of domains, OII + OI for $c_0 > 0.25$, OII + $\overline{\text{OI}}$ for $c_0 < 0.25$, gives rise, locally, to structures resembling the Magneli phases described by Khachaturyan and Morris (KM). Superficially, it may appear that the present findings confirm the KM model of "transient homologous structures". In point of fact, quite the opposite is true, as will now be shown. First note that the "method of concentration waves" as used by KM to construct the reported phase diagrams[30,31] here reduces exactly to a two dimensional Bragg-Williams model with first and second neighbor effective pair interactions. A simple back-Fourier transform of the KM mean field internal energy, for their chosen star values of $V(0)$ and $V(\mathbf{k}_1)$, immediately yields the required values (in our notation) of V_1 and V_2 (=V_3), with ratio $V_2/V_1 = -0.4286$.....The representative point of this ratio is indicated by a cross (x) on the diagonal in Fig. 2, near point #1. This ratio, inserted into the Bragg-Williams model, as expected, reproduced exactly the KM phase diagram.[32]

Next consider the "Magneli" structures proposed by KM: $[(O\square)^j O]$ where O and $\square$ represent filled and empty chains on the α sublattice respectively, where the square brackets denote periodic repetition and where the parentheses indicate that the Ortho. II element is to be repeated *j* times. Such structures are actually a subset of the well-known ground states of the one-dimensional Ising model and are stabilized by dominant *positive* (i.e. repulsive) first neighbor pair interaction J_1 along the Ising line[33,34] which is the **a** direction in orthorhombic 1-2-3. But, as mentioned above, for fully formed chains the only relevant interaction is the interchain repulsive interaction V_3 which is precisely J_1. Hence the presence of "Magneli" structures, stable or metastable, necessarily requires $J_1 \equiv V_3 > 0$. The KM phase diagram, however, is constructed with $V_2 = V_3 < 0$ so that this model is actually internally inconsistent, as was already noted earlier[4]. A check was performed by a Monte Carlo simulation employing the "symmetric" KM interaction parameters $V_2 = V_3 = -0.4286V_1$ and, as expected, no Magneli-like ordered states, stable or otherwise, were found. From the foregoing it is thus clear that *the presence of states of partial one-dimensional order necessarily implies that Ortho. II must be a stable phase in the system.*

At low temperature, the behavior of the proposed model with $V_2 > 0$ and $V_3 < 0$ is highly unusual: at $\tau \approx 0.2$, the interchain O – O correlation length is expected to become greater than the dimension of the Monte Carlo periodic cell so that spurious results may occur as discussed for example by Selke[35] in the context of the two dimensional ANNNI model. The system essentially can be mapped onto

a one-dimensional Ising model with nearest neighbor J_1 interaction for which only three ground states exist: the "ferromagnetic" (OI and $\overline{\text{OI}}$) and the "antiferromagnetic" (OII). Moreover, for $J_1 \equiv V_3 > 0$, any mixing of "ferro." and "antiferro." domains at fixed average O-concentration yields the same energy so that complete degeneracy prevails.

The mixing of domains appears to be not completely random, however. Indeed, at intermediate temperatures when the full two-dimensional character of the system is recognized by the Monte Carlo simulation, OI, $\overline{\text{OI}}$ or OII long range order (LRO) is observed at equilibrium, as expected from the phase diagram. At low-temperature, the two-dimensional character of the model is not totally absent, especially during the early stages of chain formation (see Fig. 7) so that effective long-range (entropy driven) interchain repulsion may occur. Resulting structures and their Fourier transforms are clearly reminiscent of ordered structures and diffraction patterns observed from 1-2-3 samples annealed at low temperatures for long periods of time under reducing conditions with final oxygen stoichiometry between about $z \equiv 6.25$ and 6.75 [36]: split diffraction peaks and diffuse streaks are seen about the [1/2,0] positions, but rather sharp peaks at positions [1/3,0] and [2/3,0] indicate, however, that actual longer-range repulsive interactions, beyond V_3, may be present along the a direction.

DISCUSSION

Results from phase diagram calculations and Monte Carlo simulation appear to be in close agreement with experimental findings. Indeed, at this same conference, Professor Amelinckx[37] showed some remarkable high resolution electron micrographs and diffraction patterns which confirm the general picture which emerges from theoretical findings. The close agreement was undoubtedly facilitated by the Antwrp group's[37] use of a sample preparation technique featuring very slow cooling of $YBa_2Cu_3O_z$ samples *at constant oxygen content z* (through use of a feedback control on a thermogravimetric balance). In this way, low temperature equilibrium at fixed z could be achieved which previous quenching methods could not. With this technique, one-dimensional OI, OII and $\overline{\text{OI}}$ domains were seen in the micrographs[37], just as observed in the simulations.

Moreover, Ortho. II was clearly shown to be a stable phase. In earlier dark field electron microscopy work on quenched samples[11], only small volume fractions of Ortho. II were reported, but it was argued elsewhere[4,22] that this was probably the result of poor correlation of mirror planes along the c direction: OII domains phase shifted from plane-to-plane will project as OI thereby causing appreciable underestimation of the areal fraction of OII on each plane. With constant-concentration slow cooling, however, the plane-to-plane correlation could be made almost perfect with only occasional antiphase shifts[13]. This result may appear somewhat surprising in view of the fact that O–O effective interactions between mirror planes along c must be heavily screened by intervening ions. Close to the critical point for two dimensional ordering however, correlation lengths in each plane become infinite so that effective ordering interactions between planes may become arbitrarily large with respect to the one-dimensional faulting tendency

due to entropy[17]. Thus, by slow constant-z cooling, nearly perfect three-dimensional OII ordering may be attained. For Ortho. I there is no problem: elastic strains due to orthorhombicity make the exchange of **a** and **b** axes orientations far too costly.

The asymmetry of the proposed Ising model ($V_2 < 0$, $V_3 > 0$) guarantees the formation of very long chains along the **b** axis at low temperature, thereby leading to quasi one-dimensional states of order. High one-dimensional degeneracy also results at very low temperature as demonstrated by Monte Carlo simulation, and in agreement with the low temperature CVM calculation of Kikuchi and Choi[26]: it is seen in Fig. 5 that all low temperature transitions are second order so that a complete series of domain mixing can obtain, in no violation of the third law of thermodynamics, recent claims to the contrary notwithstanding[30,31].

The Kikuchi-Choi phase diagram appears to be the most complete to date although there are indications that more complex ordered phases may become stable at low temperatures[8,36]. Indeed, recent Monte Carlo simulations performed with $V_4/V_1 = 0.25$ (V_4 being the next nearest interchain interaction, beyond V_3) lead to stability of OO□ and O□ □ "Magneli" phases[39]. It is important to note, however, that the existence of these and other states of order is incompatible with "symmetric" ($V_2 = V_3$) miscibility gap models. With large enough V_4 (and beyond), the phase diagram of Fig. 5 of course would have to be modified.

ACKNOWLEDGEMENTS

Ground state and phase diagram calculations were performed in collaboration with A. Berera and L. T. Wille. Monte Carlo studies were performed by C.P. Burmester, M.E. Mann and L.T. Wille with programming assistance from C. Carter. Special thanks are due to Dr. R. Kikuchi who allowed the author to reproduce the phase diagram of Fig. 5. Helpful discussions were held with S. Amelinckx, G. Ceder, D.H. Lee, S. C. Moss, J. D. Jorgensen and H. Zandbergen. The research was supported by a grant from the Director, Office of Energy Research, Materials Sciences Division, U.S. Department of Energy, under contract DE-AC03-76SF00098.

REFERENCES

1. M. K. Wu, J. R. Ashburn, C. J. Torny, P. H. Hor, R. L. Meng, L. Gao, Z. J. Huang, Y. Q. Wang and C. W. Chu; Phys. Rev. Lett. 58, 908 (1987).
2. R. Beyers and T. Shaw, in "Solid State Physics," Vo. 42, H. Ehrenrich and D. Turnbull, Eds., pp. 135-212, Academic Press, NY (1989).
3. D. de Fontaine, L.T. Wille and S.C. Moss, Phys. Rev B 36, 5709 (1987).
4. D. de Fontaine, in " Proceeding of Fifth Meeting of Japanese Committee for Alloy Phase Diagrams," June 1988.
5. F. Ducastelle and F. Gautier, J. Phys. F 6, 2039 (1976).
6. L.T. Wille and D. de Fontaine, Phys. Rev. B 37, 2227, (1988).
7. G. Van Tendeloo, H.W. Zandbergen and S. Amelinckx, Sol. St. Comm. 63, 603 (1987).
8. M.A. Alario-Franco, J.J. Capponi, C. Chaillout, J. Chenevas and M. Marezio, Mat. Res. Soc. Symp. Proc. 99 (1988).

9. R.J. Cava, B. Batlogg, C.H. Chen, E.A. Rietman, S.M. Zahurak and D. Werder, Phys. Rev. B 36, 5719 (1987).
10. R.M. Fleming, L.F. Schneemeyer, P.K. Gallagher, B. Batlogg, L.W. Rupp and J.V. Waszczak (preprint).
11. C.H. Chen, D.J. Werder, L.F. Schneemeyer, P.K. Gallagher and J.V. Waszczak (preprint).
12. Y. Nakazawa, M. Ishikawa, T. Katabatake, H. Takeya, T. Shibuya, K. Terakura and F. Takei, Japanese J. Appl. Phys. 26, L682, (1987); Y. Nakazawa, M. Ishikawa, T. Katabatke, K. Koga and K. Terakura, Japanese J. Appl. Phys. 26, L798 (1987).
13. S. Amelinckx, Proceedings of this conference.
14. F. Claro and V. Kumar; Surf. Sci. 119, L371 (1982).
15. K. Binder and D.P. Landau, Phys. Rev. B 21, 1941 (1980).
16. N.C. Bartelt, T.L. Einstein and L.T. Wille (preprint).
17. D.H. Lee, private communication.
18. J. Ihm, D.H. Lee, J.D. Joannopoules and J.J. Xiong, Phys. Rev. Letters, 51, 1872 (1983)
19. Per Bak, P. Kleban, W.N. Unertl, J. Ochab, G. Akinci, N.C. Bartelt and T.L. Einstein, Phys. Rev. Letters 54, 1539 (1985).
20. R. Kikuchi, Phys. Rev. 81, 988 (1951).
21. A. Berera, L.T. Wille and D. de Fontaine, J. Stat. Phys.: Short Communication 50, 1245 (1988).
22. D. de Fontaine, in "Proc. of NATO Institute on Phase Stability," Crete, July 1987 (in press).
23. J. C. Wheeler, private communication.
24. A. Berera and D. de Fontaine, Phys. Rev. B 39, 6727 (1989).
25. E.D. Specht, C.J. Sparks, A.G. Dhere, J. Brynestad, O.B. Cavin, D.M. Kroeger and H.A. Oye, Phys. Rev. B 37, 7426 (1988).
26. R. Kikuchi and J.S. Choi (preprint).
27. L.T. Wille, A. Berera and D. de Fontaine, Phys. Rev. Lett. 60, 1065 (1988).
28. D. de Fontaine, M.E. Mann and G. Ceder, to be submitted.
29. C.P. Burmester and L.T. Wille (preprint).
30. A.G. Khachaturyan and J.W. Morris, Jr., Phys. Rev. Lett. 61, 215 (1988).
31. A.G. Khachaturyan and J.W. Morris, Jr., Phys. Rev. Lett. 59, 2776 (1987).
32. G. Ceder, unpublished work at U.C. Berkeley (1989).
33. S. Katsura and A. Narita, Prog. Th. Phys. 50, 1750 (1973); M. Kaburagi and J. Kanamori, Prog. Th. Phys. 54, 30 (1975).
34. A. Finel, These de Doctorat d'Etat, Universite Pierrre et Marie Curie, July 1987 (unpublished) and references cited therein.
35. W. Selke, Z. Physik B - Condensed Matter 43, 335 (1981).
36. R. Beyers (private communication).
37. M.E. Mann, unpublished work at U.C. Berkeley (1989).